International Journal of Electrical, Electronic and Communication Sciences
ISSN: 2517-9438
Vol:8, No:8, 2014

Electro-Thermal Imaging of Breast Phantom: An Experimental Study

H. Feza Carlak, N. G. Gencer

***Abstract*—**To increase the temperature contrast in thermal images, the characteristics of the electrical conductivity and thermal imaging modalities can be combined. In this experimental study, it is objected to observe whether the temperature contrast created by the tumor tissue can be improved just due to the current application within medical safety limits. Various thermal breast phantoms are developed to simulate the female breast tissue. In vitro experiments are implemented using a thermal infrared camera in a controlled manner. Since experiments are implemented *in vitro*, there is no metabolic heat generation and blood perfusion. Only the effects and results of the electrical stimulation are investigated. Experimental study is implemented with two-dimensional models. Temperature contrasts due to the tumor tissues are obtained. Cancerous tissue is determined using the difference and ratio of healthy and tumor images. 1 cm diameter single tumor tissue causes almost 40 °mC temperature contrast on the thermal-breast phantom. Electrode artifacts are reduced by taking the difference and ratio of background (healthy) and tumor images. Ratio of healthy and tumor images show that temperature contrast is increased by the current application.

***Keywords*—**Medical diagnostic imaging, breast phantom, active thermography, breast cancer detection.

I. Introduction

BREAST cancer is the most common cancer type among women [1]. Imaging techniques used in the determination of the masses in the breast are mammography, ultrasound, computed tomography, magnetic resonance imaging, positron emission tomography and electrical impedance tomography. However, there is no gold standard in breast cancer diagnosis. Consequently, complementary imaging modalities are used. Ultrasound is also one of the most important imaging modalities used to evaluate breast. However, it cannot show micro calcifications and cannot monitor deep areas of a breast [1].

Mammography is the standard test for breast screening, however, it has accuracy problems especially for smaller tumours and it is not comfortable for patients. If the dimension of a tumour is lower than 1.6 cm, it cannot be reliably sensed (since X-rays that pass through the tumour is less affected). Statistical studies show that there is 10-25 % false negative ratio in mammography [2]. When the patients are imaged by mammography, they are exposed to an ionizing radiation which may be harmful for the human tissue.

H. F. Carlak is with the Electrical & Electronics Engineering Department, Akdeniz University, Antalya, Turkey (phone: 90-242-2274400; fax: 90-242-3106306; e-mail: fezacarlak@akdeniz.edu.tr).

N. G. Gencer is with the Electrical & Electronics Engineering Department, Middle East Technical University, Ankara, Turkey (e-mail: ngencer@eee.metu.edu.tr).

Electrical impedance tomography and thermal infrared imaging are also used in breast cancer diagnosis. However, they are not individually sufficient to diagnose cancerous tissue in early stages. It is not easy to separate malign tissue from benign tissue with electrical impedance tomography; it needs further improvements [3]. The accuracy of tumor detection should be improved in infrared imaging, especially when the tumor is located at deeper locations and at early stages [4]. Smaller tumours cannot be detected from deeper locations. Temperature increases on the skin surface occur due to blood perfusion and metabolic heat generation of the tumor tissue. However, the temperature contrast on the breast surface due to metabolic heat generation of the cancerous tissue is not sufficient to be sensed when the tumor is located at deeper regions of the breast. It cannot produce adequate amount of temperature difference on the skin surface. The noise equivalent temperature difference of modern state-of-the-art thermal infrared cameras is approximately 20 mK, so tumor tissue should create at least this amount of temperature contrast to be detected. Due to these reasons, none of these imaging modalities is adopted as a gold standard in detecting a cancerous tissue in the breast. They have been used as an adjunct to conventional medical imaging techniques.

An innovative method is developed that increases the temperature contrasts of tumor and healthy tissue. By applying electrical currents within medical safety limits, an extra electromagnetic energy is induced inside the tissue. Creating an extra energy source, the new active mode is formed beside the existing passive mode. This new energy source generates extra temperature rises in the breast tissue. Since the electrical conductivity of cancerous tissue is more than (5-10 times) the healthy tissue, the temperature increase of the tumor will be higher compared to normal breast tissue. Thus, temperature contrast is actively increased and imaging performance will be improved, and hence, cancerous tissue can be detected at deeper locations.

In our previous studies, two- and three-dimensional realistic breast models were developed (including the cancerous tissue) to investigate the feasibility with numerical simulations. Simulations are implemented by using Comsol Multiphysics Modeling and Matlab Software Tools, and thermal images of an electrically stimulated female breast were obtained [5]. Temperature distributions are obtained both in passive and active modes for two- and three-dimensional models.

An experimental study is implemented as a continuation of the numerical feasibility study. The contribution of active mode on the temperature contrast of medical infrared cameras is investigated. Voltage controlled AC current source is used

to inject surface currents to the body phantom. Biological agar phantoms are developed which has electrically and thermally similar characteristics with the female breast tissue. Temperature distributions of the phantoms are imaged by the thermal infrared camera.

II. Problem Analysis and Experimental Study

A. Theoretical Background of the Problem

Theoretical analysis of thermal contrast enhancement with current injection is presented below. Electromagnetic problem of the method is modeled and the schematic of the electromagnetic problem is shown in Fig. 1. The electrical model of the body is represented using permeability $\mu = \mu_0$, electrical conductivity κ and permittivity ϵ. Sinusoidal currents are applied using two electrodes attached on the body surface at points A and B. Applied currents generate an electric field in the conductive body. The steady-state electric field $\vec{E} = -jw\vec{A} - \nabla\emptyset$ can be calculated using the following coupled partial differential equations,

$$\nabla^2\vec{A} - jw\mu(\kappa + jw\epsilon)\vec{A} - \mu(\kappa + jw\epsilon)\nabla\emptyset = 0 \quad (1)$$

$$\nabla.[(\kappa + jw\epsilon)\nabla\emptyset] + \nabla(\kappa + jw\epsilon).jw\vec{A} = 0 \quad (2)$$

and boundary conditions,

$$\kappa\frac{\partial\emptyset}{\partial n} = \begin{cases} I\ on\ A \\ -I\ on\ B \\ 0\ otherwise \end{cases} \quad (3)$$

where $\vec{A}$ is the magnetic vector potential, $\emptyset$ is the scalar potential, and I is the current applied from the surface.

Fig. 1 Electromagnetic model of the tissue exposed to the electric current

Thermal problem is also modeled to obtain the temperature distribution inside the tissue. Schematic of the Bio-Heat problem (including an external heat source due to current application) is shown in Fig. 2. Pennes Bio Heat Equation is used to describe the effects of metabolic generation and blood perfusion over the energy balance. It explains the thermal interaction between tissues and perfused blood in detail:

$$\rho C_h\frac{\partial T}{\partial t} + \nabla.(-k\nabla T) = Q_b + Q_{met} \quad (4)$$

where, ρ is the density (kg/m^3), C_h is the specific heat (J/kg.K), T is the absolute temperature (K), k is thermal conductivity (W/m.K), Q_b is the heat source due to blood perfusion and Q_{met} is the metabolic heat generation (W/m^3).

Law of conservation of energy states that the heat lost from the skin surface is in a constant equilibrium with the heat supplied by the vascular flow to the skin in the steady state. Thus, heat transfer from the front skin surface (by both convection and radiation to the surrounding air and surfaces at specified temperatures) should be considered as the boundary conditions:

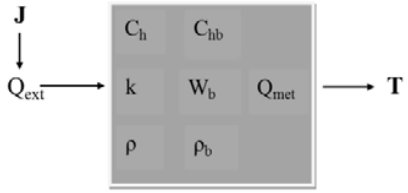

Fig. 2 Schematic of the Bio-Heat problem when electrical currents are included as heat sources

$$Q_{conv} = h_h A_s(T_S - T_\infty) \quad (5)$$

$$Q_{rad} = e\sigma A_s(T_s^4 - T_{sur}^4) \quad (6)$$

where, h_h is the convection heat transfer coefficient (W/(m^2.K)), A_s is the surface area through which the convection heat transfer takes place, T_s is the surface temperature, T_∞ is the temperature of the air, e is the emissivity of a skin (0.95), σ is the Stefan-Boltzmann constant (W/(m^2.K^4)), and T_{sur} is the temperature of the walls, ceiling and floor. In this study, T_{sur} is assumed to be equal to the air temperature ($T_{sur} = T_\infty$).

Note that, the boundary condition at the front skin surface can also be written as [6]:

$$-k\nabla T = h_h(T - T_\infty) \quad (7)$$

here, h_h (W/(m^2.K)) represents the overall heat transfer coefficient due to the combined effect of radiation and convection. To set the boundary condition at the rear surface of the breast, the temperature of the thoracic wall can be assumed to be the core temperature of the body (i.e., 310 K).

Due to the applied external current sources, a new term should be added to the right-hand side of the Pennes Bio Heat equation:

$$\rho C_h\frac{\partial T}{\partial t} + \nabla.(-k\nabla T) = Q_b + Q_{met} + Q_{ext} \quad (8)$$

The external heat term Q_{ext} is calculated using the following Joule Heat Equation:

$$Q_{ext} = \frac{1}{\kappa}|J|^2 \quad (9)$$

where J is the electrical current density and κ is the electrical conductivity of the tissue. However, the experimental study is implemented with a biological phantom. Since it is not a live tissue, all terms in the equation drop except the Q_{ext}.
Therefore, heat occurs due to the current application and (8) turns out to be:

$$\nabla.(-k\nabla T) = Q_{ext} \quad (10)$$

B. Experimental Study

Long-wave band uncooled microbolometer camera was used in experiments. Fig. 3 shows the experimental setup performed using the micro bolometer infrared camera in the Biophysics Department Laboratories. The properties of the camera are given in detail in Table I.

TABLE I
CHARACTERISTICS OF THE INFRARED CAMERA USED IN EXPERIMENTS

Detector type	Microbolometer
Resolution (pixels)	320x240
Dynamic range (bit)	14
Spectral range (μm)	7.5-13
NETD (at 30°C)	40 mK
Detector cooling	Uncooled
Integration time (msec)	12
Used frame rate (Hz)	9
Max frame rate (Hz)	50 at full frame
Focus distance (cm)	100

Experiments are carried out in a temperature controlled room (approximately at 23°C). Current, within medical safety limits, is applied to the phantom with the voltage controlled current generator. The phantom which simulates the female breast is modelled using agar, TX-150, TX-151, distilled water and saline (NaCl) to adjust the conductivity of the healthy breast and cancerous tissue [7]. The focal distance between the camera and phantom is adjusted as 1 m.

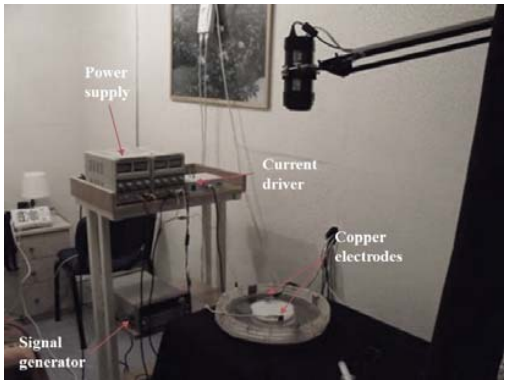

Fig. 3 Experimental setup of Electro-Thermal Imaging System established at Faculty of Medicine, Biophysics Department

1. Model Preparation

One of the best materials that mimic the electrical dielectric property of the woman breast tissue is the agar phantom. It resembles the electrical impedance characteristics of the human tissue in the frequency range of 1 kHz to 10 MHz [8]. For this purpose, an agar phantom is designed with two-compartments (Fig. 4). The background of the phantom simulates the healthy tissue. On the other hand, inner tissue which is inserted into the background phantom imitates the malignant tissue. Adjusting the saline ratio of the phantom, electrical conductivity of the model can be altered. So, it is possible to produce different types of tissues such as healthy and malignant breast tissues. Agar powder, the basic component of the phantom, is used to prevent the decomposition of water. The electrical conductivity is adjusted by changing the sodium chloride (NaCl) ratio of the solution. The following expression shows the relationship between the amount of ingredients and the resulting electrical conductivity of the phantom [9]:

$$S=2\ \rho\ (S/m) \quad (11)$$

where S is the conductivity of the phantom and ρ shows the amount of NaCl which will be poured into the solution to be able to obtain the desired electrical conductivity. In this formulation, it is assumed that 1.5 gr agar is added into 100 ml distilled water.

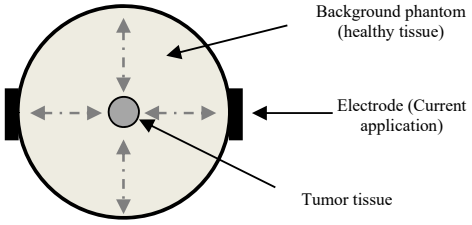

Fig. 4 Phantom geometry: electrodes are inserted to the right and left side boundaries. Background phantom simulates the healthy breast tissue and inner tissue (its location can be moved) mimics the tumor tissue

To increase the viscosity and to ensure better mixing of the solution, jellying agent TX-150 and TX-151 are used [7]. TX-151 is a new product of TX-150. Since it is improved with preservatives, it has longer shelf life [10]. Since a number of specifications must be satisfied simultaneously, preparation of experimental phantoms is a difficult process. For example, phantoms should be rigid enough to preserve their shape. They should not dry out or decompose quickly to keep their electrical properties constant. Some stable phantom compositions used in our experimental studies are presented in Table II.

TABLE II
PHANTOM INGREDIENTS AND CORRESPONDING CONDUCTIVITY VALUES

Ingredients	Healthy Tissue 1	Healthy Tissue 2	Healthy Tissue 3	Cancerous Tissue
Distilled Water (ml)	100	100	100	100
Agar (gr)	1.5	1	3	1.5
TX-150 (gr)	---	1	---	---
TX-151(gr)	---	---	1	---
Sucrose (gr)	---	---	---	1.5
NaCl (gr)	0.1	0.05	0.05	0.2
Conductivity (S/m)	0.2	0.1	0.16	1

2. Experimental Process

In this study, a pair of electrodes is attached on the surface of the agar phantoms and alternating current is applied from the surface electrodes. In the experimental studies, there are no metabolic heat sources and blood perfusion. Thus only the

effects of electrical current application can be observed here. Moreover, the physical (density and specific heat of tissue), electrical (electrical conductivity and permittivity of tissue) and thermal properties (thermal emissivity and conductivity of tissue) of the phantom cannot be adjusted exactly the same with real breast tissue parameters. Consequently, some differences in results (temperature increases and contrasts) must be expected compared to simulation results. Different experiments are performed by changing the location and the dimension of the cancerous tissue. Thermal images are acquired for each case and temperature distributions of the phantoms are obtained in active and passive mode of operation.

III. Results & Discussion

A. Homogeneous Phantom Study

In this study, 10 mA (10 kHz) current was applied for 600 msec. Fig. 5 denotes the 2-D phantom used in this part of the study. Two-dimensional healthy breast tissue was modeled with a circular homogeneous phantom which has 8 cm diameter. The electrical conductivity of the tissue was adjusted as 0.2 S/m. The temperature distribution of the agar phantom was imaged both in passive and active modes. Difference of two images (see Fig. 6) was obtained and the average background temperature was calculated to observe the effects of the current application. A temperature contrast of 0.092 ˚C occurs on the phantom due to the applied current.

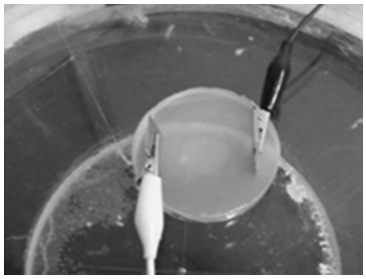

Fig. 5 Homogeneous agar phantom: Current is applied with copper electrodes located at right and left side of the phantom

B. Inhomogeneous Phantom Study

In this part, 10 mA (10 kHz) current was applied for 600 msec. Healthy breast tissues was modeled with a circular phantom which has a 10 cm diameter. The malignant tissue was simulated as a smaller circular region which has a 1 cm diameter. Tumor tissue was placed 1 cm away from the surface electrode (Fig. 7). Almost 40°mC temperature contrast occurs due to the tumor tissue in the active mode. The difference of homogeneous and inhomogeneous phantom images is shown in Fig. 8. The ratio of these images is shown Fig. 9. A noticeable temperature contrast was obtained in the figure. Since there is no metabolic heat generation, temperature contrast does not occur in passive mode. One can benefit greatly from electrical conductivity of the tissues being different from each other (cancerous tissue has higher electrical conductivity compared to the healthy tissue). Due to this phenomenon, the tumor tissue can be detected using an infrared thermal camera**.**

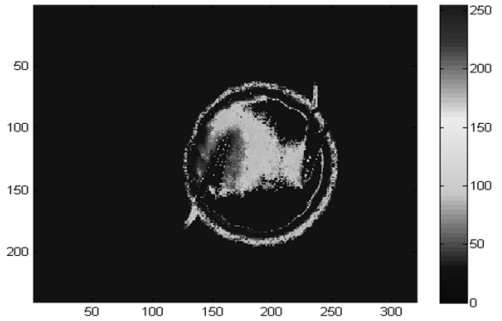

Fig. 6 Difference of images (taken in active and passive mode) (Using micro bolometer uncooled thermal infrared camera: Color bar indicates the temperature difference (°mC)

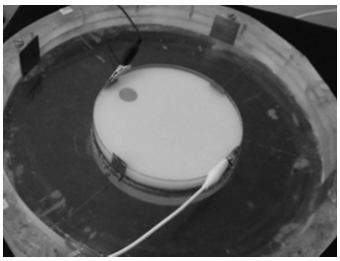

Fig. 7 Agar phantom including an inhomogeneity representing the tumor tissue: Electrodes are attached at the boundary of the phantom

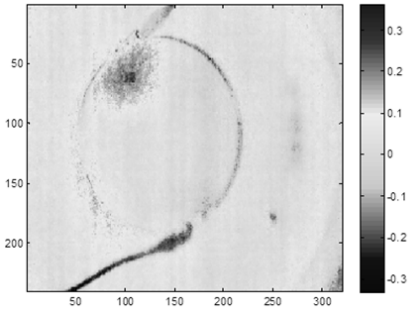

Fig. 8 Differences of healthy and tumor tissue images (Using micro bolometer uncooled thermal infrared camera (spatial resolution is 320 x 240 pixels). Color bar indicates the temperature difference (°C)

In experiments, applied current was within the medical safety limits and expected temperature contrasts were around 100 °mC according to the simulation results. Since infrared cameras are used to image the temperature distributions, temperature contrasts should be in the range of thermal sensitivity of the cameras. The NETD of the uncooled microbolometer camera (used in experiments) is 40 mK. Tissue phantom stayed immobile during the experiments (about 10 minutes) so integration times of the cameras did not reduce the thermal sensitivity. The pixel number of the uncooled microbolometer camera is 320×240. The phantom used for the healthy (10 cm diameter) and the malignant tissue (1 cm diameter) were circular models. When the camera is

focused on the phantom, the field of view (FOV) of the uncooled microbolometer camera is 10x10 cm (corresponding to a 0.031 cm × 0.041 cm pixel size). Thus, the pixel size of the camera is much smaller than the area of tumor tissue (1x1 cm) which is sufficient to follow the temperature contrasts of the malignant tissue. The main components of the in vitro experimental study are thermal-body phantom, a current generator and a thermal camera. Voltage-controlled AC current source (VCCS) is used to supply constant current into the breast phantom independent of the load specifications.

The emissivity of the designed phantom (0.95-0.98) resembles the tissue emissivity. The dimension of the circular phantom (a diameter of 10 cm) was also adjusted to be consistent with the realistic breast model (a half sphere with a 14 cm diameter). Body phantom was composed of two compartments which were healthy and cancerous tissue. Since cancerous tissue has a higher electrical conductivity compared to the malignant tissue, NaCl is used to adjust the electrical conductivity of the different tissues.

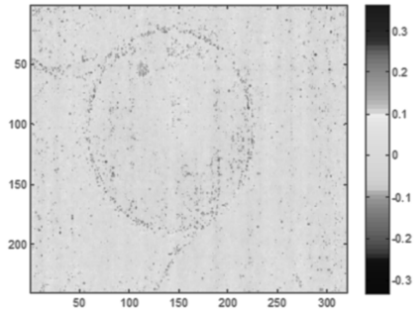

Fig. 9 Ratio of healthy and tumor tissue images (Using microbolometer uncooled thermal infrared camera (spatial resolution is 320 x 240 pixels). Color bar indicates the temperature difference (°C)

In the first part of the experiments, the difference image of the active and passive (no heating occurs) modes was obtained and temperature contrast due to current application was calculated. Applied current causes 92°mC temperature increase on the homogeneous body phantom.

Second part of the experiments was carried out by applying an AC excitation at 10 kHz. Tumor tissue was detected by taking the difference and ratio images of homogeneous and inhomogeneous phantom temperature distributions. Tumor tissue created almost 40°mC temperature contrast in AC mode of operation. Another important result was removing the electrode artifacts in large extent by taking the ratio of images.

Temperature contrasts were detected both in the ratio of thermal images taken in active and passive modes and ratio of the healthy and tumor tissue images. However, image resolution was better in the ratio of images taken in active and passive modes compared to the ratio of the healthy and tumor tissue images. Although current artifacts were disappeared by taking the ratio of images; deviations in the phantom, registration errors and changes in the experimental conditions may cause extra artifacts. Even if tumors were located close to each other, boundaries of the tumors were distinctive and image resolution of the thermal image was almost same with image of the single tumor. Temperature contrasts of each tumor tissue can be clearly sensed with the infrared camera.

Since there are no heat sources (metabolic heat source) or blood perfusion affecting the thermal-body phantom, experimental studies show the bare effect of the current application on temperature contrast. Results show that applying currents in the medical safety limits enhances the temperature contrast in substantial amounts that can make the invisible tumors visible.

ACKNOWLEDGMENT

F. Carlak thanks to Dr. Murat Ozgoren and his colleagues for giving me an opportunity to use their camera and laboratory at 9 Eylul University, Medical Faculty, Biophysics Department, Izmir.

REFERENCES

[1] H. Qi, N. A. Diakides, 2003, “Thermal Infrared Imaging in Early Breast Cancer Detection – A Survey of Recent Research,” IEEE Embs 25th Annual International Conference, pp. 1109-1112.
[2] M. Morrow, R. Schmidt, B. Cregger and C. Hasset, 1994, “Preoperative Evaluation of Abnormal Mammographic Findings to Avoid Unnecesssary Breast Biopsies,” Arch. Surg., 129, pp. 1091-1096.
[3] S. Prasad N, D. Houserkova, J. Campbell, 2008, “Breast Imaging Using 3d Electrical Impedence Tomography,” Biomed Pap Med Fac Univ Palacky Olomouc Czech Repub, 152, pp. 151–154.
[4] Z. Deng, J. Liu, 2005, “Enhancement of Thermal Diagnostics on Tumors Underneath the Skin by Induced Evaporation,” Proceedings of the 2005 IEEE Engineering in Medicine and Biology 27th Annual Conference.
[5] H. F. Carlak, N. G. Gençer, C. Beşikçi, 2011, “Medical Thermal Imaging of Electrically Stimulated Woman Breast: a simulation study, IEEE Engineering in Medicine and Biology Society Conference (EMBS 11)
[6] T. R. Gowrishankar, D. A. Stewart, G. T. Martin, J. C. Weaver, 2004, “Transport lattice models of heat transport in skin with spatially heterogeneous, temperature-dependent perfusion,” Biomedical Engineering Online, 3:42, pp. 1-17.
[7] W. M. A. Ibrahim, 2008, “Short Review on the Used Recipes to Simulate the Bio-Tissue at Microwave Frequencies,” Biomed 2008, Proceedings 21, pp. 234-237.
[8] G. Qiao, W. Wang, L. Wang, Y. He, B. Bramer and M. Al-Akaidi, 2007, “Investigation of biological phantom for 2D and 3D breast EIT images,” IFMBE Proceedings 17, pp. 328–331.
[9] B. Ülker, 2001, “Electrical Conductivity Imaging via Contactless Measurements: An Experimental Study,” Master’s Thesis, METU.
[10] TX Products Catalogue, Oilcenter.